iScience

CellPress
OPEN ACCESS

Article

MTFR2 shapes a barrier of immune microenvironment in hepatocellular carcinoma

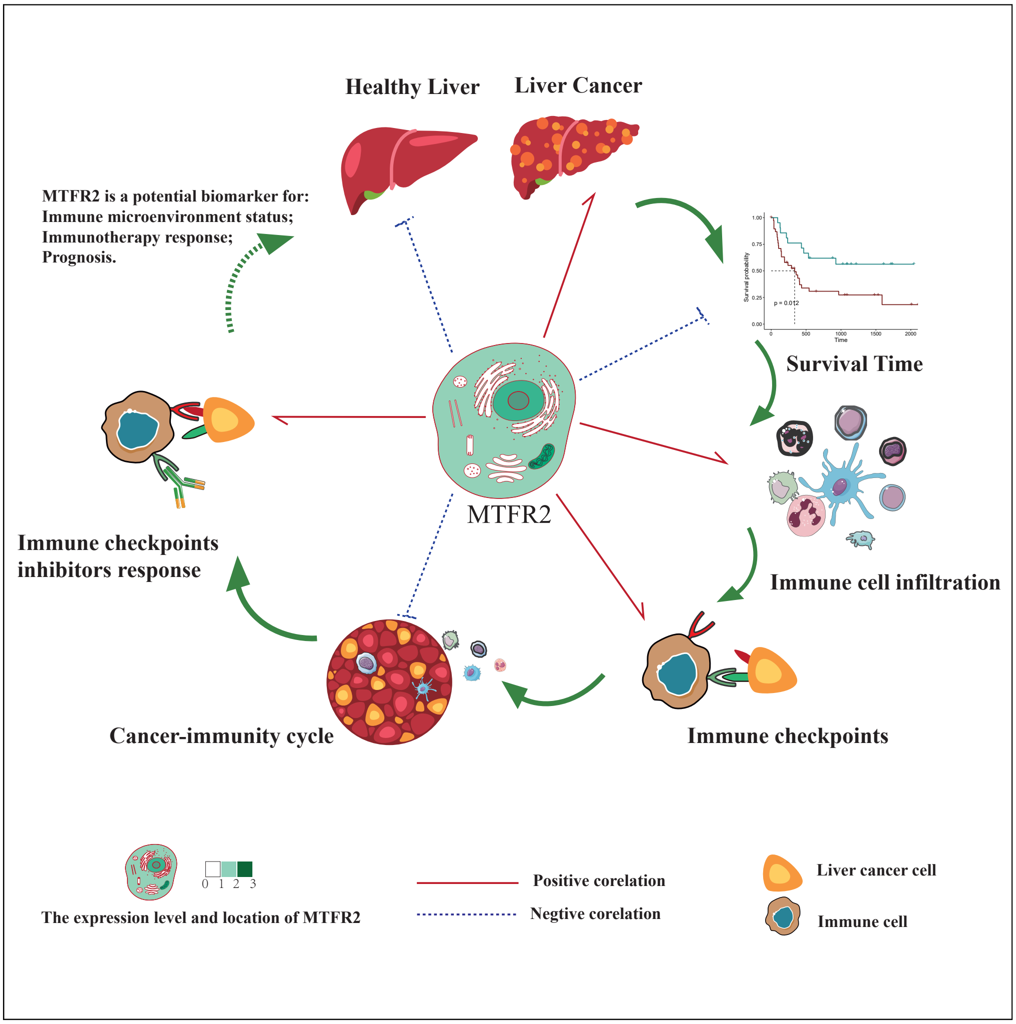

Qiaoqiao Huang, Ying Han, Edward Shen, ..., Shan Zeng, Changjing Cai, Hong Shen

vccj07@csu.edu.cn (C.C.)
hongshen2000@csu.edu.cn (H.S.)

Highlights

MTFR2 is upregulated in HCC, leading to shorter OS and worse DFS in patients

MTFR2 is positively related with immune cell infiltration level and immune checkpoints

MTFR2 may act as an important role in cancer-immunity cycle

MTFR2 can shape a barrier of immune microenvironment, but may be broken by immunotherapy

Huang et al., iScience *26*, 105095
January 20, 2023
https://doi.org/10.1016/j.isci.2022.105095

iScience

CellPress OPEN ACCESS

Article

MTFR2 shapes a barrier of immune microenvironment in hepatocellular carcinoma

Qiaoqiao Huang,[1,2,5] Ying Han,[1,2,5] Edward Shen,[3] Ziyang Feng,[1,2] Yinghui Peng,[1,2] Le Gao,[1,2] Yan Gao,[1,2] Yongting Liu,[1,2] Wei Li,[1,2] Ping Liu,[1,2] Yihong Chen,[1,2] Cao Guo,[1,2] Shan Zeng,[1,2,4] Changjing Cai,[1,2,*] and Hong Shen[1,2,4,6,*]

SUMMARY

Hepatocellular carcinoma (HCC) is a leading cause of cancer-related death in the world. Mitochondrial fission regulator 2 (MTFR2) is involved in the development of various cancers. However, the roles of MTFR2 in HCC remain unknown. In this study, we conducted a comprehensive analysis of MTFR2 in HCC, which was generated from integrative MTFR2 analyses of eight HCC cell lines, and three datasets (public dataset, real-world dataset, and immunotherapy dataset) derived from bulk HCC tissues, survival, and immunotherapy data. We demonstrated that the expression level of MTFR2 is upregulated in HCC, leading to poor prognosis. MTFR2 is positively correlated with the level of immune cell infiltration, multiple immune checkpoints and immunotherapy response prediction pathways, and acts as an important role in cancer-immunity cycle. In conclusion, our work indicates that MTFR2 can shape a barrier of immune microenvironment and result in poor prognosis in hepatocellular carcinoma, but the immune barrier may be broken by immunotherapy.

INTRODUCTION

Hepatocellular carcinoma (HCC) has the seventh highest incidence worldwide and the second highest mortality rate among cancers. Asia is the region with the second highest incidence of primary HCC (Mcglynn et al., 2021). The prognosis of HCC is pretty poor because of the limitations of treatments. Fortunately, immune checkpoint inhibitors (ICI) have shown inspiring efficacy in HCC (Chen et al., 2019; Liu et al., 2021; Rimassa et al., 2019). However, only a few patients can benefit from an ICI treatment. Therefore, there is an urgent need to identify some biomarkers that can predict the immunotherapy response of patients with HCC, reveal resistance mechanisms, and seek potential targets for enhancing immunotherapy efficacy (Cheu and Wong, 2021; Li et al., 2019; Ruf et al., 2021).

Mitochondrial fission regulator 2 (MTFR2), also known as family with sequence similarity 54, member A (FAM54A), is mainly located in mitochondrial membranes and vesicles, which can promote mitochondrial fission and play a role in aerobic respiration (Lu et al., 2020). MTFR2 has been reported to be associated with a poor prognosis of HCC based on the data of TCGA, but without the real-world validation (Li et al., 2021). What's more, previous studies have shown that MTFR2 plays a significant role in the immune microenvironment of gastric cancer and breast cancer. The study by Zhu et al. showed that the expression level of MTFR2 was negatively correlated with the infiltration of B cells, $CD8^+$ T cells, $CD4^+$ T cells, macrophages, neutrophils, and dendritic cells in gastric cancer, and also showed obvious correlation with CD19, CD79A, CCL2, CCR7, BDCA-4, and other immune markers (Zhu et al., 2021). Wang et al. found out that MTFR2 was positively correlated with the infiltration levels of B cells, neutrophils, and dendritic cells in breast cancer and negatively correlated with the infiltration of CD4+T cells, CD8+T cells, and macrophages (Wang et al., 2020). However, the role of MTFR2 in the immune microenvironment of HCC remains largely unknown.

In this study, we conducted a comprehensive analysis of MTFR2 in HCC, which was generated from integrative MTFR2 analysis of HCC cell lines and three datasets (TCGA dataset, real-world survival validation dataset and real-world immunotherapy dataset) derived from bulk HCC tissues, survival data, and immunotherapy response data. First, we evaluated the expression level of MTFR2 in HCC and its correlation with

[1]Department of Oncology, Xiangya Hospital, Central South University, Changsha, Hunan 410008, China

[2]Key Laboratory for Molecular Radiation Oncology of Hunan Province, Xiangya Hospital, Central South University, Changsha, Hunan 410008, China

[3]Department of Life Science, McMaster University, Hamilton, ON L8S 4L8, Canada

[4]National Clinical Research Center for Geriatric Disorders, Xiangya Hospital, Central South University, Changsha, Hunan 410008, P.R. China

[5]These authors contributed equally

[6]Lead contact

*Correspondence: vccj07@csu.edu.cn (C.C.), hongshen2000@csu.edu.cn (H.S.)

https://doi.org/10.1016/j.isci.2022.105095

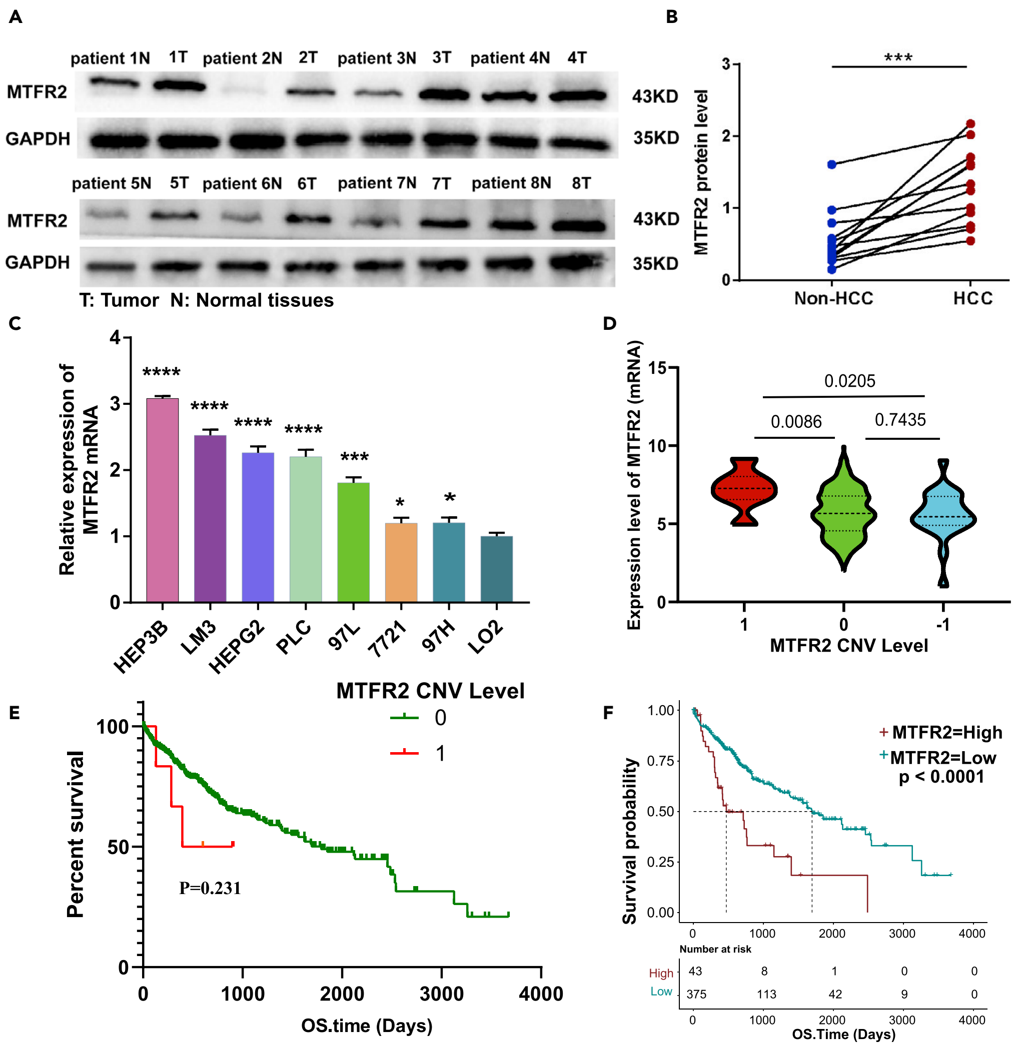

Figure 1. MTFR2 results in the poor prognosis of hepatocellular carcinoma

(A and B) MTFR2 protein levels in paired HCC samples and adjacent non-tumor liver (n = 12) (*p < 0.05; **p < 0.01; ***p < 0.001).

(C) MTFR2 mRNA levels in 7 human HCC cell lines and human hepatocyte cell line. Data were mean ± SD and from three independent experiments.

(D–F) CNV pattern of MTFR2 in HCC. (−1: single copy deletion, 0: diploid normal copy, 1: low-level copy number amplification) (F) Kaplan–Meier curves comparing the overall survival (OS) in patients with HCC with low and high MTFR2 expression in TCGA-LIHC cohort (log rank test).

the prognosis of patients with HCC. Then, we performed the analysis of MTFR2 in the immune microenvironment. Lastly, we evaluated the potential role of MTFR2 in the immunotherapy response. Our work explored the potential importance of MTFR2 as a new predictive biomarker for prognosis and immunotherapy response in HCC.

RESULTS

MTFR2 results in the poor prognosis of hepatocellular carcinoma (TCGA dataset and real-world dataset)

To investigate the role of MTFR2 in regulating HCC progression, we first examined MTFR2 protein levels in 12 paired HCC and adjacent non-tumor tissues. Our data showed that the protein levels of MTFR2 were significantly upregulated in HCC tissues when compared with the matched adjacent non-tumor tissues (Figures 1A, S1C). We then examined the MTFR2 mRNA levels in human hepatocyte cell line (LO2)

Table 1. Univariate and Multivariate Cox regression analysis of OS in TCGA Cohort

		Univariate Cox		Multivariate Cox	
Clinical feature	Group	HR (95% CI)	P-Value	HR (95% CI)	P-Value
Age	≤60	1	0.76	1	0.94
	>60	1.06(0.72–1.56)		0.986(0.676–1.44)	
Gender	Male	1	0.638	1	0.646
	Female	0.93(0.67–1.27)		0.929(0.678–1.27)	
Stage	I-II	1	<0.001	1	<0.001
	III-IV	1.8(1.3–2.51)		1.96(1.42–2.7)	
MTFR2	High	1	<0.001	1	<0.001
	Low	0.44(0.28–0.68)		0.39(0.255–0.596)	

and seven human HCC cell lines (Hep3B, HepG2, Huh-7, MHCC97-H, HCCLM3, SMMC-7721, and PLC/PRF/5) by performing RT-qPCR analysis. The results obtained show that the expression of MTFR2 in the seven HCC cell lines was higher than that of human hepatocyte cell line (LO2) (Figure 1C). Next, we collected data from the TCGA database to detect the copy number variation (CNV) pattern of MTFR2 in HCC. The results obtained show that copy number amplification was the main cause of MTFR2 mRNA expression upregulation, and it also resulted in shorter survival (Figures 1D and 1E). Meanwhile, the surv_cutpoint algorithm was used to obtain the best MTFR2 expression cut-off value for survival (Cut-off value: 1.355165). Kaplan-Meier survival analysis indicated that patients with high MTFR2 expression had shorter overall survival (OS) time and a worse prognosis than those with low MTFR2 expression (Figure 1F). In addition, in order to further explore the prognostic effect of MTFR2 expression in HCC, we used Cox proportional hazards regression model to analyze prognostic factors. All patients with HCC were classified according to the expression level of MTFR2 (MTFR2 high-expression group and MTFR2 low-expression group). Univariate analysis showed that high MTFR2 expression was associated with poor OS time. Multivariate analysis showed that the expression of MTFR2 was independently correlated with OS time. The above results indicate that MTFR2 can be a predictor of the prognosis of patients with HCC (Table 1).

To further verify the potential effect of MTFR2 on HCC, we conducted a retrospective study as the real-world dataset. Immunohistochemical results showed that MTFR2 expression level in HCC tissues was significantly higher than that in adjacent normal tissues. (Figure S1B) According to the results of immunohistochemistry, the expression level of MTFR2 was divided into high-expression group and low-expression group according to the best cut-off value from the surv_cutpoint algorithm (Cut-off value: 3 IHC score). The results obtained show that patients with high MTFR2 expression had poorer OS and disease-free survival (DFS) than those with low MTFR2 expression (Figures 2A–2C). Similarly, we used the cox proportional hazards regression model to analyze prognostic factors. The samples in the validation cohort were classified according to the expression level of MTFR2 (MTFR2 high-expression group and MTFR2 low expression group). The results were consistent with the previous results: univariate analysis showed that high MTFR2 expression was associated with poor OS time; multivariate analysis showed that MTFR2 expression was independently related to OS time (Table 2).

The different expression genes between high- and low-MTFR2 group

To explore the possible mechanisms of MTFR2 in HCC, we identified the different expression genes (DEGs) between the high- and low-MTFR2 groups (Figures 3A and 3B). The results of GO analysis obtained show that DEGs were significantly enriched in multiple immune functions and the seven functions with the highest enrichment were humoral immune response, regulation of humoral immune response, humoral immune response mediated by circulating immunoglobulin, regulation of humoral immune response mediated by circulating immunoglobulin, immunoglobulin-mediated immune response, regulation of inflammatory response, and acute inflammatory response (Figure 3C). Furthermore, KEGG analysis showed that DEGs were enriched in multiple immune-related signaling pathways and the pathways with the highest enrichment were inflammatory mediator regulation of TRP channels, human T cell leukemia virus 1 infection, cytokine-cytokine receptor interaction, AMPK signaling pathway, and p53 signaling pathway (Figure 3D). These results suggest that MTFR2 may play an important role in HCC.

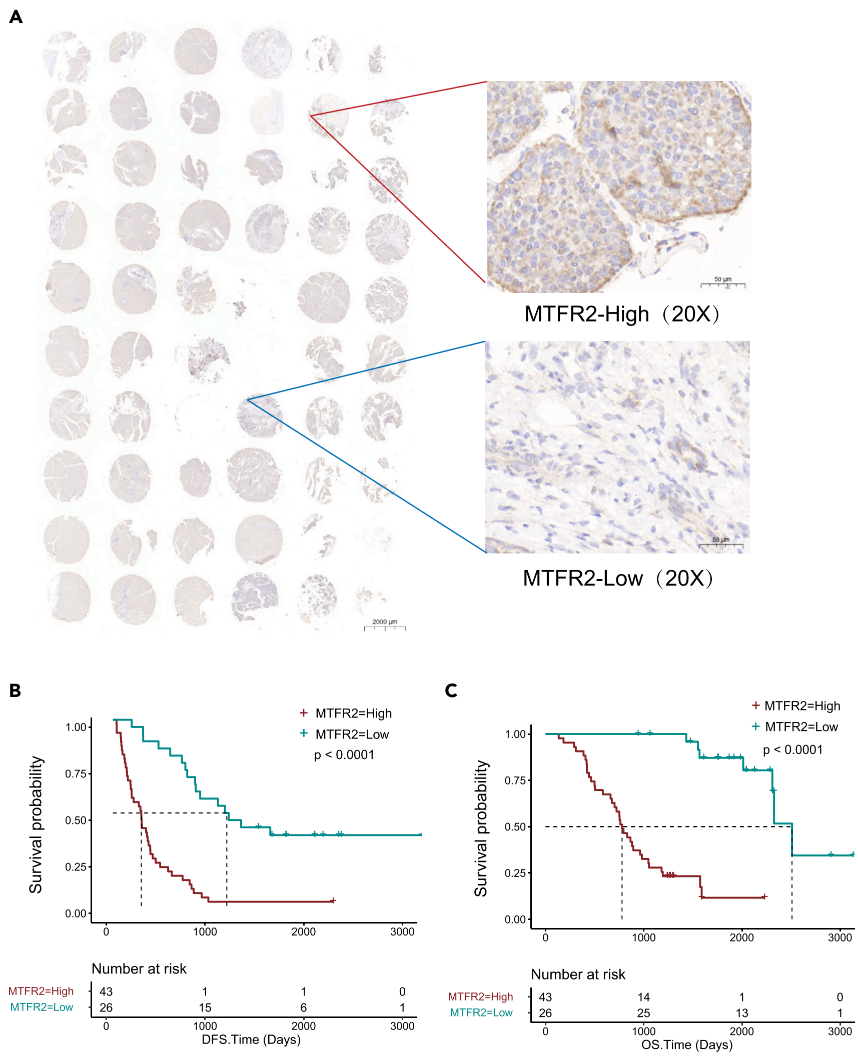

Figure 2. MTFR2 results in the poor prognosis of hepatocellular carcinoma

(A) The expression level of MTFR2 in the tissue array.

(B and C) Kaplan–Meier curves comparing the overall survival (OS) and relapse-free survival (RFS) in HCC patients with low and high MTFR2 expression in the retrospective cohort (log rank test).

MTFR2 shapes a barrier of immune microenvironment in hepatocellular carcinoma

In order to investigate the role of MTFR2 in the immune microenvironment of HCC, we used the TIMER and GEPIA databases to assess the level of immune infiltration of HCC. The results obtained from the TIMER database show that MTFR2 expression level had a significant positive correlation with the levels of B cell (cor. = 0.455, $p < 0.0001$), $CD8^+$ T cell (cor. = 0.353, $p < 0.0001$), $CD4^+$ T cell (cor. = 0.283, $p < 0.0001$), macrophage (cor. = 0.427, $p < 0.0001$), neutrophil (cor. = 0.364, $p < 0.0001$), and dendritic cell infiltration (cor. = 0.436, $p < 0.0001$) in liver hepatocellular carcinoma (LIHC) (Figure 4A).

Next, we further explored the correlation between the expression level of MTFR2 and different immune cell immune marker sets in the GEPIA database to verify the results of the TIMER database analysis. According to the results obtained, immune markers of $CD8^+$ T cells, $CD4^+$ T cell, B cells, M1 macrophages, M2 macrophages, neutrophils, and dendritic cells were positively correlated with MTFR2 expression in LIHC. In addition, in the GEPIA database, the immune markers of T cell (general), monocyte, tumor-associated macrophage, T helper 1 (Th1) cell, Th2 cell, Th17 cell, T follicular helper cell (Tfh), regulatory T cell (Treg), natural killer cell, and T cell exhaustion also showed positive correlations with MTFR2 expression levels (Table S1).

Table 2. Univariate and Multivariate Cox regression analysis of OS in Real-world Cohort

		Univariate Cox		Multivariate Cox	
Clinical feature	Group	HR (95% CI)	P-Value	HR (95% CI)	P-Value
age	≤60	1	0.625	1	0.406
	>60	1.17(0.618–2.22)		0.75(0.38–1.48)	
gender	Male	1	0.438	1	0.704
	Female	1.34(0.643–2.77)		0.87(0.41–1.81)	
stage	I-II	1	<0.001	1	0.003
	III-IV	4.3(2.15–8.59)		2.94(1.44–6.00)	
MTFR2	High	1	<0.001	1	<0.001
	Low	0.0653(0.022–0.193)		0.07(0.02–0.23)	

Since MTFR2 expression is positively correlated with immune activation characteristics, we further used the TISIDB database to analyze MTFR2 expression and TILs, immunosuppressive agents, immunostimulatory factors, chemokines, chemokine-receptors, and major histocompatibility complexes (MHCs). The results of TIL showed that the levels of $CD4^{+}$ T cell, $CD8^{+}$ T cell, Th2 cell, natural killer T cell, Tfh cell, and myeloid-derived suppressor cell infiltration were positively correlated with MTFR2 expression, and the $CD4^{+}$ T cell infiltration level had the strongest correlation (cor. = 0.588, $p < 0.0001$). In contrast to the GEPIA results, the levels of Th1 cell, eosinophil, immature dendritic cell, monocyte, natural killer cell, and plasmacytoid dendritic cell were negatively related with MTFR2 expression and eosinophil had the strongest correlation (cor. = −0.229, $p < 0.0001$) (Figure 4B).

The results of immunoinhibitor analysis revealed that MTFR2 expression positively correlated with seven of eight immunoinhibitors' expressions. Among them, cytotoxic T-lymphocyte-associated antigen 4 (CTLA4) had the strongest correlation coefficient (cor. = 0.337, $p < 0.0001$). Furthermore, MTFR2 expression negatively correlated with kinase insert domain receptor (KDR) (cor. = −0.482, $p < 0.0001$) (Figure 4C). Immunostimulator analysis showed that MTFR2 expression was positively correlated with most immunostimulators' expression (19/25), and tumor necrosis factor receptor superfamily 18 (TNFRSF18) had the most significant positive correlation (cor. = 0.349, $p < 0.0001$). In addition, six immunostimulators had negative correlations, and interleukin 6 receptor (IL6R) had the strongest correlation (cor. = −0.245, $p < 0.0001$) (Figure 4D).

Chemokine analysis showed that MTFR2 expression was positively correlated with C-C motif chemokine ligand 4 (CCL4), CCL13, CCL20, CCL26, CCL28, C-X-C motif chemokine ligand 3 (CXCL3), CXCL5, CXCL13, CXCL17, and X-C motif chemokine ligand 1(XCL1), XCL2. XCL had the strongest correlation (cor. = 0.303, $p < 0.0001$). Additionally, MTFR2 expression was negatively correlated with CCL2, CCL14, CCL15, CCL16, CCL21, CCL23, CXCL2, CXCL12, and C-X3-C motif chemokine ligand 1 (CX3CL1), and CCL14 had the strongest correlation (cor. = −0.519, $p < 0.0001$) (Figure 4E).

Chemokine receptor analysis revealed that all C-C chemokine receptor (CCR) family members and MTFR2 expression were positively correlated, and CCR10 had the strongest correlation (cor. = 0.279, $p < 0.0001$). As for the C-X-C motif chemokine receptor (CXCR) family, CXCR3, CXCR4, and CXCR6 were positively correlated with the expression of MTFR2. CXCR1 and CXCR2 were negatively correlated with the expression of MTFR2. CX3CR1 was negatively correlated with the expression of MTFR2 as well. Among them, CXCR1 had the strongest correlation (cor. = −0.201, $p < 0.0001$) (Figure 4F).

MHC analysis showed that MTFR2 expression was positively correlated with human leukocyte antigen-DO beta (HLA-DOB) and HLA-DQA2 and antigen peptide transporter 1 (TAP1), and TAP1 had the strongest correlation (cor. = 0.233, $p < 0.0001$). However, B-2 microglobulin (cor. = −0.233, $p = 0.00618$) and HLA-E (cor. = −0.222, $p = 0.00618$) were negatively correlated with MTFR2 expression (Figure 4G).

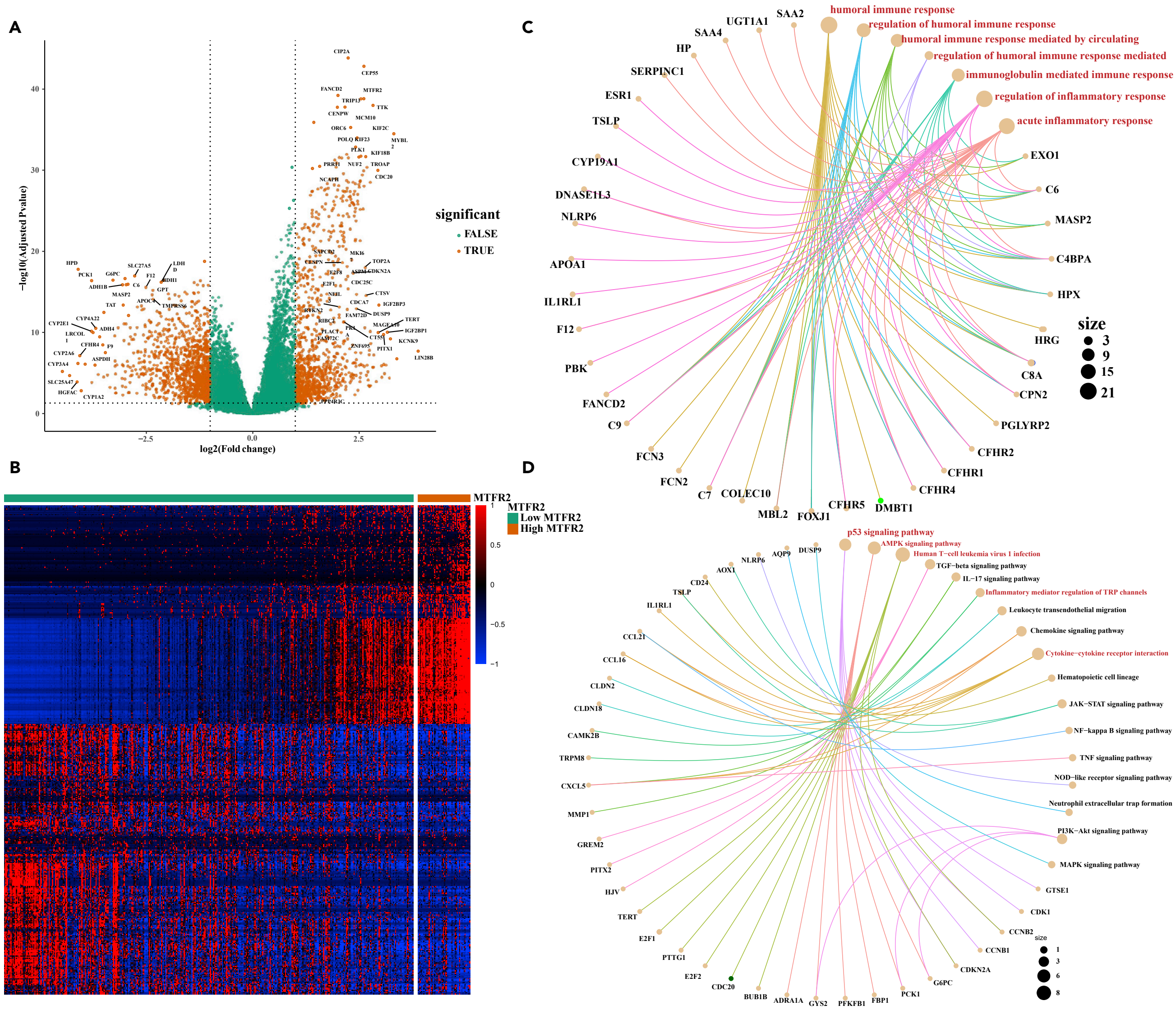

Figure 3. The different expression genes between high and low MTFR2 group

(A and B) GEO and TCGA analysis identified the different expression genes (DEGs) between the high- and low-MTFR2 groups.
(C–D) GO and KEGG analysis of the DEGs between high- and low-MTFR2 groups.

MTFR2 may induce immune barrier of HCC via immune checkpoint

MTFR2 was found to be positively correlated with a majority of immune checkpoints including CTLA4, LAG3, LAIR1, TIGIT, NECTIN2, CD274, CD276, ADORA2A, BTLA, VSIR, CD200, CD200R1, CD80, CD86, HAVCR2, IDO1, LGALS3, PDCD1, and PVR (Figures 5A and 5B). To further explore the association between MTFR2 and immunity, a correlation analysis was conducted between MTFR2 and cancer-immunity cycle. As shown in Figure 5C, in the high-MTFR2 group, two steps in the cycle were found to be upregulated, including the release of cancer cell antigens (Step 1) and NK cell recruiting (Step 4). Furthermore, the activities of T cell recruiting (Step 4), Th2 cell recruiting (Step 4), and infiltration of immune cells into tumors (Step 5) were downregulated in the high-MTFR2 group. In addition, MTFR2 was found to be positively correlated with the most immunotherapy-predicted pathways, including base excision repair, DNA replication, cell cycle, pyrimidine metabolism, viral carcinogenesis, p53 signaling pathway, mismatch repair, and cytokine receptor interaction (Figures 5E and 5F). As we know, $CD8^+$ T cells are the main effector cells of immunotherapy, and the immune checkpoint PD1 and PDL1 is currently the most important clinical immunotherapy target. Therefore, we verified the correlation between the expression level of MTFR2

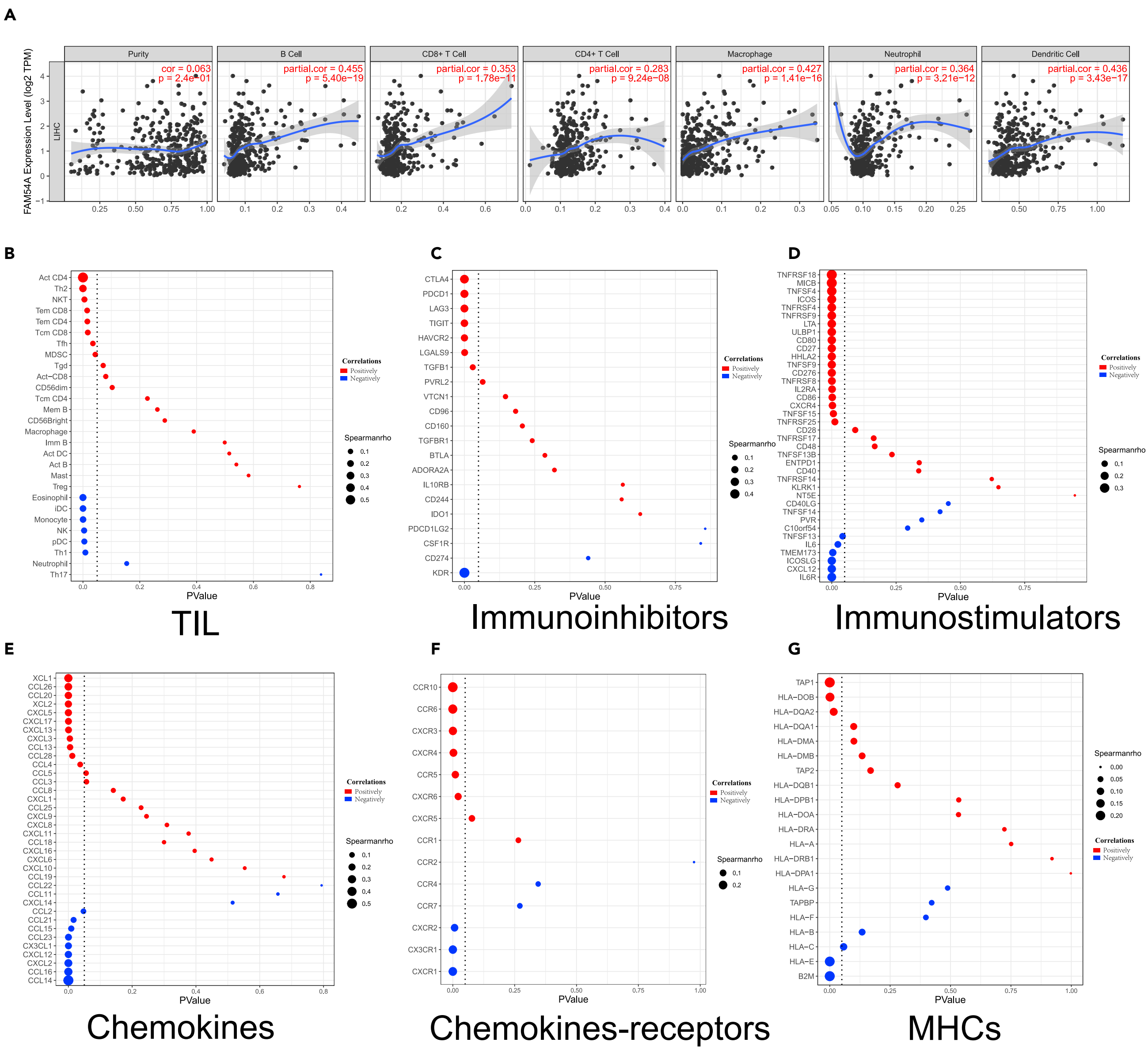

Figure 4. MTFR2 shapes a barrier of immune microenvironment in hepatocellular carcinoma

(A) The immune infiltrate analysis in the TIMER dataset.

(B) The immune infiltrate analysis in the TISIDB dataset.

(C) The correlation of MTFR2 and immunoinhibitors in the TISIDB dataset.

(D) The correlation of MTFR2 and immunostimulators in the TISIDB dataset.

(E) The correlation of MTFR2 and chemokines in the TISIDB dataset.

(F) The correlation of MTFR2 and chemokine receptors in the TISIDB dataset.

(G) The correlation of MTFR2 and MHCs in the TISIDB dataset. (Spearman coefficients test).

and the infiltration levels of CD8^{+} T cells, PD1, and PDL1 in the tumor microenvironment. The results demonstrated that the expression level of MTFR2 was positively correlated with the expression levels of CD8, PD1, and PDL1. At the same time, the expression level of CD8 and PD1/PDL1 in the high-MTFR2 group was higher than that in the low-MTFR2 group. (Figures 6A–6I).

MTFR2 is a potential biomarker for immunotherapy response

The predictive value of MTFR2 in the immunotherapy validation cohort was investigated. We retrospectively analyzed the data of 7 patients who received anti-PD-1 immunotherapy (immune checkpoint

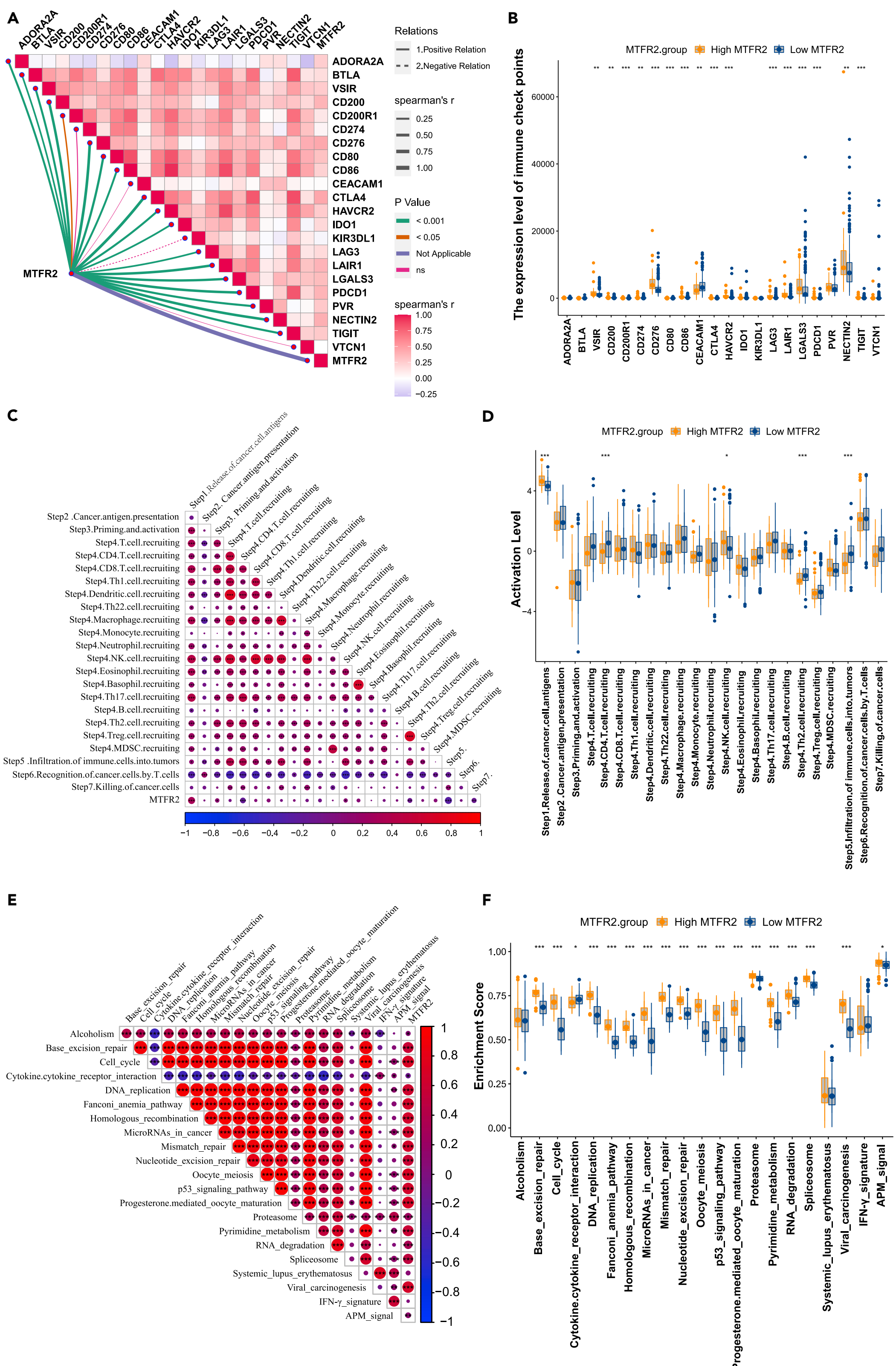
A
Relations
1.Positive Relation
2.Negative Relation
spearman's r
P Value
< 0.001
< 0.05
Not Applicable
ns
MTFR2
ADORA2A
BTLA
VSIR
CD200
CD200R1
CD274
CD276
CD80
CD86
CEACAM1
CTLA4
HAVCR2
IDO1
KIR3DL1
LAG3
LAIR1
LGALS3
PDCD1
PVR
NECTIN2
TIGIT
VTCN1
B
MTFR2.group High MTFR2 Low MTFR2
The expression level of immune check points
C
D
MTFR2.group High MTFR2 Low MTFR2
Activation Level
E
F
MTFR2.group High MTFR2 Low MTFR2
Enrichment Score

CellPress
OPEN ACCESS

Figure 5. MTFR2 may induce immune barrier of HCC via immune checkpoint

(A and B) Correlation between MTFR2 and immune checkpoints. The color and the values indicate the Spearman correlation coefficient. The asterisks indicated a statistically significant p value calculated using Kruskal-Wallis test (*$p < 0.05$; **$p < 0.01$; ***$p < 0.001$).

(C and D) Correlations between MTFR2 and the steps of the cancer immunity cycle.

(E and F) Correlations between MTFR2 and immunotherapy-predicted pathways. (Spearman coefficients test).

inhibitor, ICI). The tumor response was evaluated by CT scan results. In this cohort, 4 cases were progressive disease (PD) and 3 cases were partial response. The results obtained show that among the 7 patients with HCC who received anti-PD-1 antibody therapy, patients with high expression of MTFR2 tend to have better immunotherapy effects and better progression-free survival (Figures 7A and 7B). Meanwhile, we further confirmed the relationships between MTFR2 and immune checkpoints/immunotherapy-predicted pathways in the RNA-Seq data of the immunotherapy dataset. MTFR2 was positively correlated with most of the immune checkpoints and immunotherapy-predicted pathways (Figures 7C and 7D). Due to the insufficient number of cases, the P-value was not statistically significant, but there is a positive correlation trend.

Meanwhile, we performed some analyses between MTFR2 and some clinical biomarkers for immunotherapy response. We calculated neutrophil-to-lymphocyte ratio (NLR), peripheral blood-derived neutrophil-to-lymphocyte ratio (dNLR), lymphocyte-to-monocyte ratio (LMR), and platelet-to-lymphocyte ratio (PLR), which were identified as clinical biomarkers for immunotherapy response. The results showed that patients with high LMR had better immunotherapy response and patients with low NLR, dNLR, and PLR had better immunotherapy responses. The correlation between MTFR2 and serum immune markers has also been analyzed, but due to insufficient sample size, the result was not statistically significant (Figures 8A–8C).

DISCUSSION

In this study, by integrating expression data from RNA-Seq and lab experiments in cell lines and tumor tissues, as well as clinical information from public databases, real-world survival validation dataset and real-world immunotherapy dataset, we have shown the landscape of MTFR2 in HCC. We have demonstrated that the expression level of MTFR2 is upregulated in HCC, leading to shorter OS and worse DFS in patients. Functional enrichment analysis showed that MTFR2 is related to a variety of immune functions and immune-related signaling pathways. TIMER and GEPIA databases analyses revealed that the expression level of MTFR2 is positively correlated with the level of immune cell infiltration in the HCC tumor microenvironment, which promotes the immune response of tumor tissues. Furthermore, we found out that MTFR2 is positively correlated with multiple immune checkpoint inhibitors and immunotherapy response prediction pathways, and can promote the release of cancer cell antigens and the recruitment of NK cells while inhibiting the recruitment of T cells and Th2 cells. Finally, the immunotherapy validation cohort analysis showed that in the patients with higher MTFR2 expression levels, the immune barrier can be broken and a better immunotherapy response can be gotten.

MTFR2 may promote tumor development and cause bad prognosis via the cross-talk with immune microenvironment. Chemokine analysis showed that MTFR2 had the strongest positive correlation with XCL1, and the strongest negative correlation with CCL14. Studies have shown that the XCL1-XCR1 axis contributes to the progression of breast cancer, epithelial ovarian cancer, non-small-cell lung cancer, and oral squamous cell carcinoma (Do and Cho, 2020). Multiple studies have shown that CCL14 is related to the immune infiltration of hepatocellular carcinoma and is a prognostic marker of HCC (Gu et al., 2020; Zhu et al., 2019; Jiang et al., 2021). Chemokine receptor analysis showed that all CCR families were positively correlated with MTFR2 expression, of which CCR10 had the strongest correlation. Studies have shown that CCR10 can stimulate the occurrence of hepatocellular carcinoma and is expected to become a potential therapeutic target for inflammation-driven HCC (Wu et al., 2018). MHC analysis showed a positive correlation between MTFR2 and TAP1. TAP1 is related to tumor immune escape, and high expression of TAP1 is a poor prognostic factor for patients with stage I/II colorectal cancer (Ling et al., 2017). MTFR2 is positively correlated with the expression of most immune checkpoints such as CTLA4, LAG3, LAIR1, TIGIT, NECTIN2, CD274, and CD276. CTLA4 has been proven to promote the progression and metastasis of colorectal cancer, head and neck squamous cell carcinoma, renal cell carcinoma, lung cancer, and breast cancer (Imazeki et al., 2021; Yu et al., 2016; Zhang et al., 2019). LAG3 is expressed on tumor-infiltrating lymphocytes (TIL) and mediates T cell depletion. It has been reported that the high

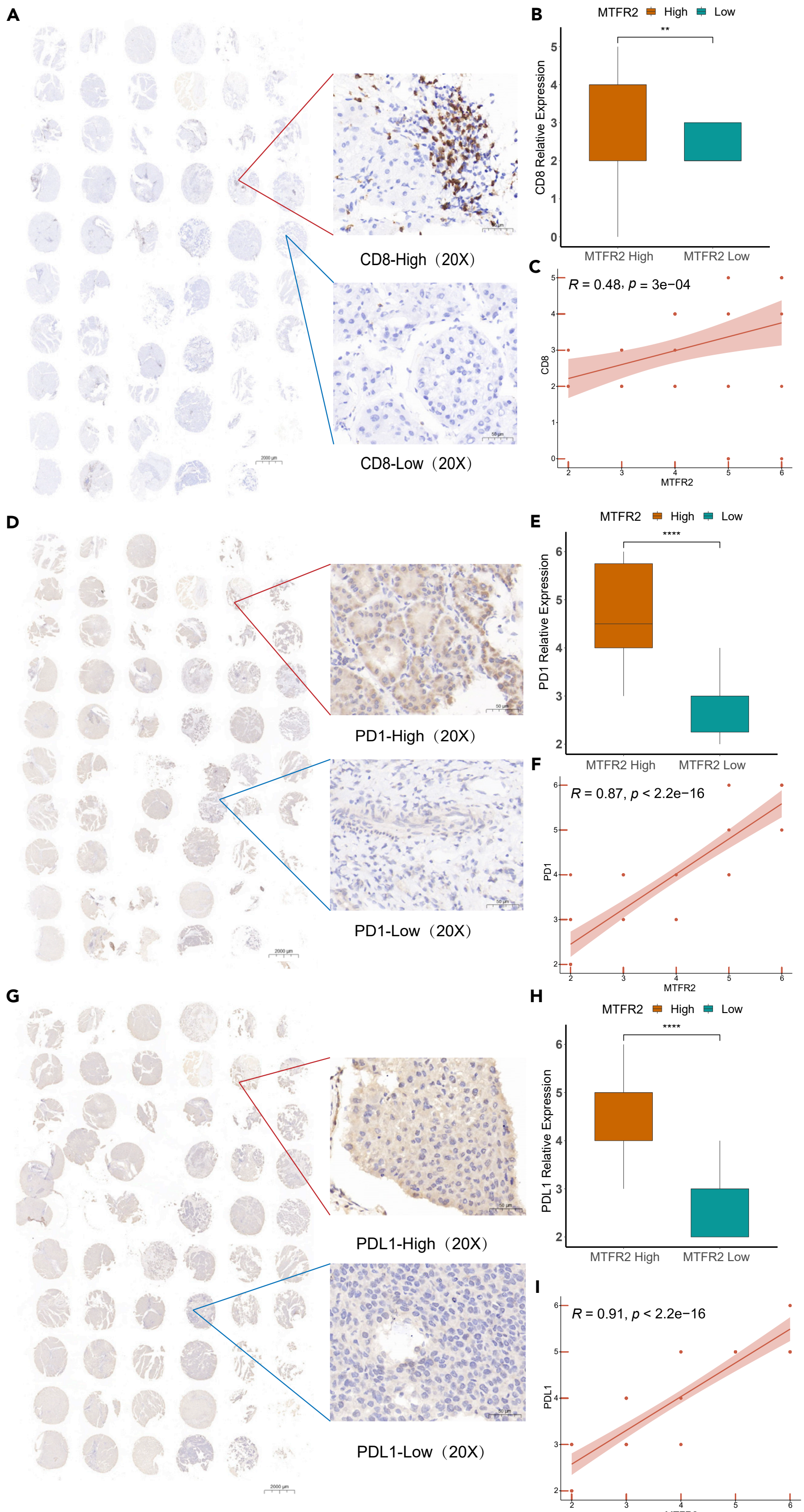
A
CD8-High（20X）
CD8-Low（20X）
B
MTFR2 High Low
CD8 Relative Expression
MTFR2 High
MTFR2 Low
C
R = 0.48, p = 3e−04
CD8
MTFR2
D
PD1-High（20X）
PD1-Low（20X）
E
PD1 Relative Expression
F
R = 0.87, p < 2.2e−16
PD1
G
PDL1-High（20X）
PDL1-Low（20X）
H
PDL1 Relative Expression
I
R = 0.91, p < 2.2e−16
PDL1

Figure 6. MTFR2 may induce immune barrier of HCC via immune checkpoint

(A–C) The correlation between MTFR2 and CD8$^+$ T cells infiltration was detected by IHC.

(B–F) The correlation between MTFR2 and PD1 was detected by IHC.

(G–I) The correlation between MTFR2 and PDL1 was detected by IHC. (*p < 0.05; **p < 0.01; ***p < 0.001. student's t test).

expression of LAG3 can affect the survival of salivary gland cancer (Arolt et al., 2020). TIGIT is mainly expressed on T cells and natural killer cells. It acts as an inhibitory checkpoint receptor, thereby limiting adaptive and innate immunity. Studies have shown that high expression of TIGIT can inhibit the function

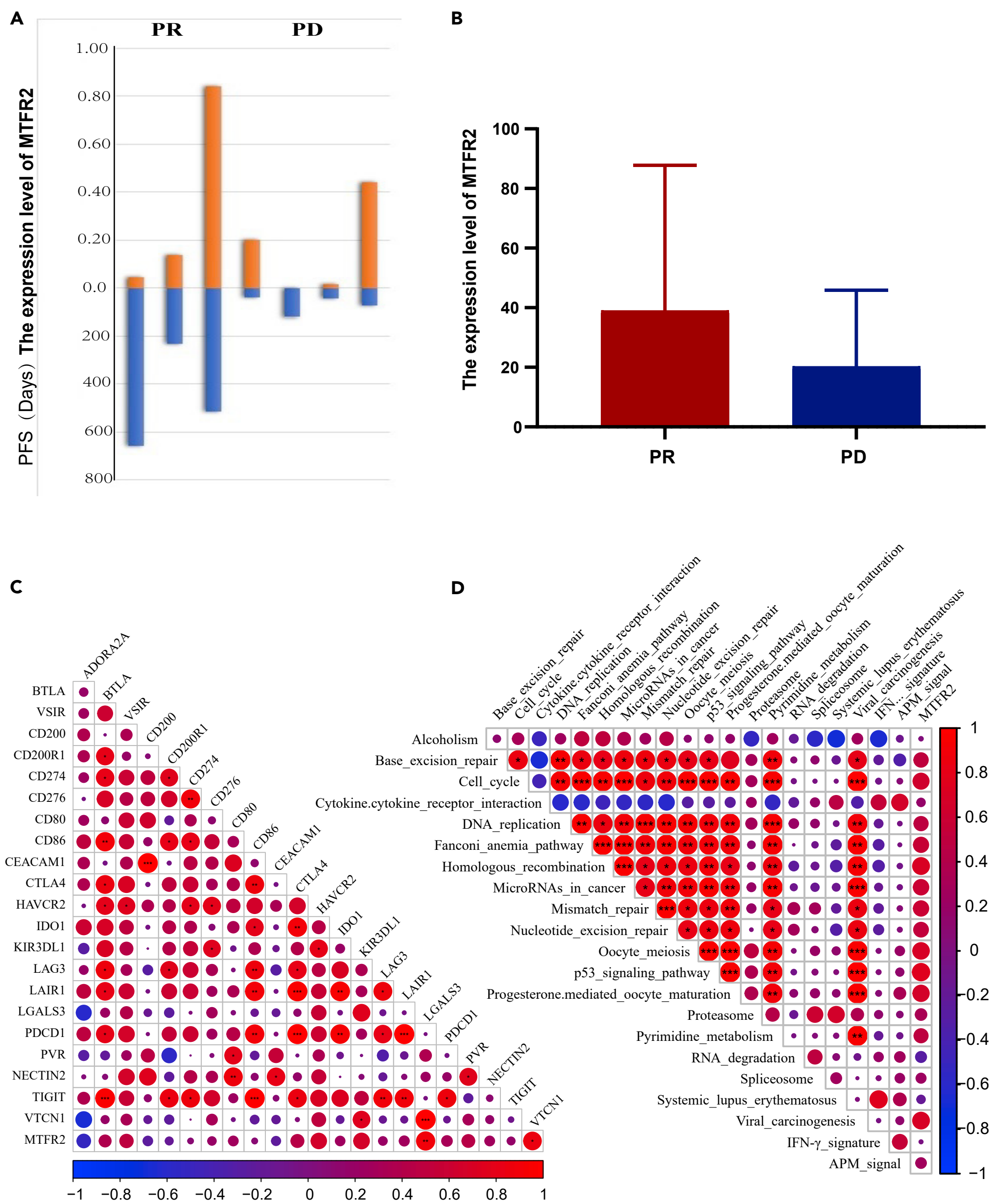

Figure 7. MTFR2 is a potential biomarker for immunotherapy response

(A and B) The effect of MTFR2 expression levels on the efficacy of anti-PD-1 immunotherapy cohorts.

(C) Correlations between MTFR2 and immune checkpoints in the RNA-Seq data of immunotherapy dataset.

(D) Correlations between MTFR2 and immunotherapy-predicted pathways in the RNA-Seq data of immunotherapy dataset. The asterisks indicate a significant statistical p value calculated using the Kruskal-Wallis test (*p < 0.05; **p < 0.01; ***p < 0.001).

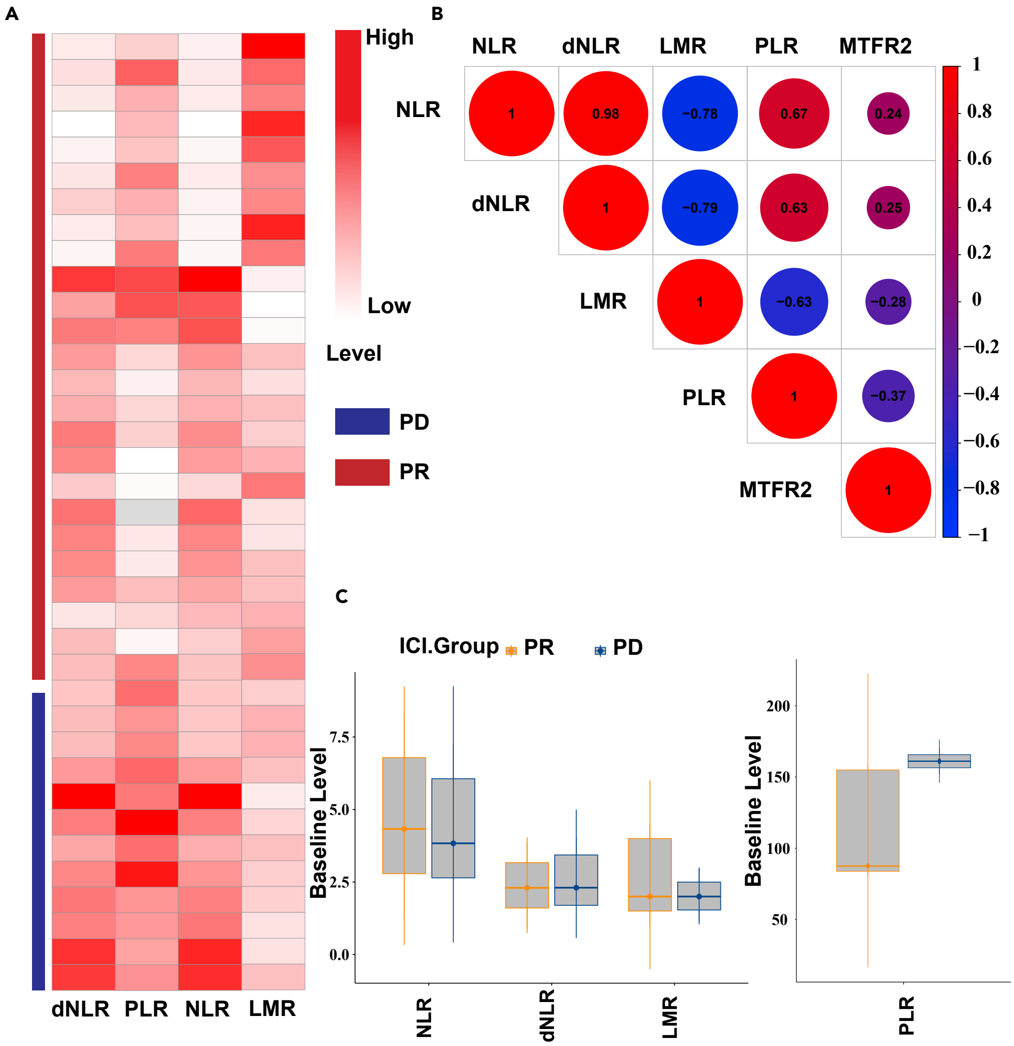

Figure 8. MTFR2 is a potential biomarker for immunotherapy response

(A) Correlations between serum immune markers and immunotherapy response.

(B) Correlations between MTFR2 and serum immune markers.

(C) Correlations between serum immune markers and immunotherapy response in the immunotherapy validation cohort.

of infiltrating CD8$^+$ T cells, thereby causing GC cells to escape immune killing (Xu et al., 2020). The binding of leukocyte-associated immunoglobulin-like receptor 1 (LAIR1) to its ligand leads to the loss of immune function in the tumor microenvironment and the decrease of T cell function and immune response of antigen-presenting cells. It has been reported that high expression of LAIR-1 can promote the occurrence of renal cell carcinoma, ovarian cancer, oral cancer, and so on (Liu et al., 2020; Nguyen et al., 2021; Jingushi et al., 2019). NECTIN2, CD274, and CD276 are overexpressed in a variety of tumors and are associated with poor prognosis (Stamm et al., 2018; Masugi et al., 2017; Wang et al., 2021). In a word, MTFR2 may induce immune barrier of HCC via immune checkpoint, which inhibits the function of infiltration immune cell and cause poor prognosis in HCC.

On the other hand, our results revealed that the expression level of MTFR2 is positively correlated with the level of HCC immune infiltration, including CD8$^+$ T cells, CD4$^+$ T cells, B cells, macrophages, neutrophils, and dendrites cells. Meanwhile, the patients with high MTFR2 seem to get better response in ICI therapy, which indicates the immune barrier can be broken by ICI therapy. In the analyses of cancer-immunity cycle, we found high expression of MTFR2 inhibits the recruitment of T cells, reducing the infiltration of immune cells into tumors, resulting in a poor prognosis for patients, which may due to the inhibition effect of immune checkpoints. Using ICI therapy, such as blocking PD-1 or its ligand PD-L1 can reactivate T cell function, which can achieve a better therapeutic effect on these patients (Xia et al., 2019). At the same time, there are many connections between MTFR2 and MHCs, which are complex; further research works are needed.

In conclusion, by integrating expression data from RNA-Sep and lab experiments, as well as clinical information from public databases, real-world survival validation dataset, and real-world immunotherapy dataset, we showed the landscape of MTFR2 in HCC. Our work indicates that MTFR2 shapes a barrier of the immune microenvironment and results in a poor prognosis in hepatocellular carcinoma. What's more, MTFR2 is a potential biomarker for immunotherapy response.

Limitations of the study

The specific mechanism by which MTFR2 affects the response to immunotherapy in HCC remains to be further explored. According to the DEGs enrichments, cytokine-cytokine receptor interaction maybe the key pathway, especially in the process of the infiltration of immune cells into tumors, which is an interesting aspect for further research. Meanwhile, the sample of immunotherapy dataset is small, large scale of cohort is needed.

STAR★METHODS

Detailed methods are provided in the online version of this paper and include the following:

- KEY RESOURCES TABLE
- RESOURCE AVAILABILITY
  - Lead contact
  - Materials availability
  - Data and code availability
- EXPERIMENTAL MODEL AND SUBJECT DETAILS
  - Patients, follow-up and Ethics
  - Cell cultures
- METHOD DETAILS
  - Western blot
  - Real-time qPCR
  - Immunohistochemistry (IHC)
  - RNA sequencing of immunotherapy cohort
  - Immunotherapy response biomarkers
  - Public data source
  - Processing of RNA-Seq data
  - Evaluation of the immunological characteristics
- QUANTIFICATION AND STATISTICAL ANALYSIS

SUPPLEMENTAL INFORMATION

Supplemental information can be found online at https://doi.org/10.1016/j.isci.2022.105095.

ACKNOWLEDGMENTS

This study was supported by grants from the National Key R&D Program of China (No. 2018YFC1313300), National Natural Science Foundation of China (No.: 81372629, 81772627, 81874073, 81974384 & 82173342), key projects from the Nature Science Foundation of Hunan Province (No. 2021JJ31092 & 2021JJ31048), the projects from Beijing CSCO Clinical Oncology Research Foundation (No. Y-HR2019-0182, Y-2019Genecast-043), and the Fundamental Research Funds of Central South University (2020zzts273, 2019zzts797).

AUTHOR CONTRIBUTIONS

Conceptualization, Q.H., Y.H., H.S., and C.C.; Methodology, Q.H., C.C., Y.H., E.S., and Z.F.; Investigation, H.P., L.G., Y.G., T.L., W.L., P.L., and C.G.; Writing – Original Draft, Q.H. and C.C.; Writing – Review & Editing, H.S. and C.C.; Funding Acquisition, Y.H., H.S., and C.C.; Resources, Q.H., Y.H., C.C., and Y.P.; Supervision, H.S. and C.C.

DECLARATION OF INTERESTS

None of the authors have any potential financial conflicts of interest related to this manuscript.

Received: February 25, 2022
Revised: May 31, 2022
Accepted: September 4, 2022
Published: January 20, 2023

REFERENCES

Arolt, C., Meyer, M., Ruesseler, V., Nachtsheim, L., Wuerdemann, N., Dreyer, T., Gattenlöhner, S., Wittekindt, C., Buettner, R., Quaas, A., and Klussmann, J.P. (2020). Lymphocyte activation gene 3 (Lag3) protein expression on tumor-infiltrating lymphocytes in aggressive and Tp53-mutated salivary gland carcinomas. Cancer Immunol. Immunother. *69*, 1363–1373. https://doi.org/10.1007/S00262-020-02551-6.

Cai, C., Peng, Y., Shen, E., Wan, R., Gao, L., Gao, Y., Zhou, Y., Huang, Q., Chen, Y., Liu, P., et al. (2022). Identification of tumour immune infiltration-associated Snornas (Tiisno) for predicting prognosis and immune landscape in patients with colon cancer via A Tiisno score model. EBioMedicine *76*, 103866–104606. https://doi.org/10.1016/J.Ebiom.2022.103866.

Chen, S., Cao, Q., Wen, W., and Wang, H. (2019). Targeted therapy for hepatocellular carcinoma: challenges and opportunities. Cancer Lett. *460*, 1–9. https://doi.org/10.1016/J.Canlet.2019.114428.

Cheu, J.W., and Wong, C.C. (2021). Mechanistic Rationales Guiding Combination hepatocellular carcinoma therapies involving immune checkpoint inhibitors. Hepatology *74*, 2264–2276. https://doi.org/10.1002/Hep.31840.

Do, H.T.T., and Cho, J. (2020). Involvement of the Erk/Hif-1α/Emt pathway in Xcl1-induced migration of Mda-Mb-231 and Sk-Br-3 breast cancer cells. Int. J. Mol. Sci. *22*, 158. https://doi.org/10.3390/Ijms22010089.

Gu, Y., Li, X., Bi, Y., Zheng, Y., Wang, J., Li, X., Huang, Z., Chen, L., Huang, Y., and Huang, Y. (2020). Ccl14 is A prognostic biomarker and correlates with immune infiltrates in hepatocellular carcinoma. Aging (Albany Ny) *12*, 784–807. https://doi.org/10.18632/Aging.102656.

Imazeki, H., Ogiwara, Y., Kawamura, M., Boku, N., and Kudo-Saito, C. (2021). Cd11b(+)Ctla4(+) myeloid cells are A key driver of tumor evasion in colorectal cancer. J. Immunother. Cancer *9*, 138. https://doi.org/10.1136/jitc-2021-002841.

Jiang, Z., Xing, C., Wang, P., Liu, X., and Zhong, L. (2021). Identification of therapeutic targets and prognostic biomarkers among chemokine (C-C motif) ligands in the liver hepatocellular carcinoma microenvironment. Front. Cell Dev. Biol. *9*, 748269–749124. https://doi.org/10.3389/Fcell.2021.748269.

Jingushi, K., Uemura, M., Nakano, K., Hayashi, Y., Wang, C., Ishizuya, Y., Yamamoto, Y., Hayashi, T., Kinouchi, T., Matsuzaki, K., et al. (2019). Leukocyte-associated immunoglobulin-like receptor 1 promotes tumorigenesis in Rcc. Oncol. Rep. *41*, 1293–1303. https://doi.org/10.3892/or.2018.6875.

Li, D., Ji, Y., Guo, J., and Guo, Q. (2021). Upregulated expression of Mtfr2 as A Novel biomarker predicts poor prognosis in hepatocellular carcinoma by bioinformatics analysis. Future Oncol. *17*, 3187–3201. https://doi.org/10.2217/Fon-2020-1160.

Li, T., Fan, J., Wang, B., Traugh, N., Chen, Q., Liu, J.S., Li, B., and Liu, X.S. (2017). Timer: a web server for comprehensive analysis of tumor-infiltrating immune cells. Cancer Res. *77*, E108–E110. https://doi.org/10.1158/0008-5472.Can-17-0307.

Li, Z., Wu, T., Zheng, B., and Chen, L. (2019). Individualized precision treatment: targeting Tam in Hcc. Cancer Lett. *458*, 86–91. https://doi.org/10.1016/J.Canlet.2019.05.019.

Ling, A., Löfgren-Burström, A., Larsson, P., Li, X., Wikberg, M.L., Öberg, Å., Stenling, R., Edin, S., and Palmqvist, R. (2017). Tap1 down-regulation elicits immune escape and poor prognosis in colorectal cancer. OncoImmunology *6*, 13561433–E1357127. https://doi.org/10.1080/2162402x.2017.1356143.

Liu, H.T., Jiang, M.J., Deng, Z.J., Li, L., Huang, J.L., Liu, Z.X., Li, L.Q., and Zhong, J.H. (2021). Immune checkpoint inhibitors in hepatocellular carcinoma: current progresses and challenges. Front. Oncol. *11*, 737497–737581. https://doi.org/10.3389/fonc.2021.737497.

Liu, Y., Ma, L., Shangguan, F., Zhao, X., Wang, W., Gao, Z., Zhou, H., Qu, G., Huang, Y., An, J., et al. (2020). Lair-1 suppresses cell growth of ovarian cancer cell via the Pi3k-Akt-Mtor pathway. Aging (Albany Ny) *12*, 16142–16154. https://doi.org/10.18632/aging.103589.

Lu, W., Zang, R., Du, Y., Li, X., Li, H., Liu, C., Song, Y., Li, Y., and Wang, Y. (2020). Overexpression of Mtfr2 predicts poor prognosis of breast cancer. Cancer Manag. Res. *12*, 11095–11102. https://doi.org/10.2147/cmar.s272088.

Masugi, Y., Nishihara, R., Yang, J., Mima, K., Da Silva, A., Shi, Y., Inamura, K., Cao, Y., Song, M., Nowak, J.A., et al. (2017). Tumour Cd274 (Pd-L1) expression and T cells in colorectal cancer. Gut *66*, 1463–1473. https://doi.org/10.1136/gutjnl-2016-311421.

Mcglynn, K.A., Petrick, J.L., and El-Serag, H.B. (2021). Epidemiology of hepatocellular carcinoma. Hepatology *73*, 4–13. https://doi.org/10.1002/hep.31288.

Nguyen, C.T., Caruso, S., Maillé, P., Beaufrère, A., Augustin, J., Favre, L., Pujals, A., Boulagnon-Rombi, C., Rhaiem, R., Amaddeo, G., et al. (2021). Immune profiling of combined hepatocellular-cholangiocarcinoma reveals distinct subtypes and activation of gene signatures predictive of response to immunotherapy. Clin. Cancer Res. *76*. https://doi.org/10.1158/1078-0432.ccr-21-1219.

Rimassa, L., Pressiani, T., and Merle, P. (2019). Systemic treatment options in hepatocellular carcinoma. Liver Cancer *8*, 427–446. https://doi.org/10.1159/000499765.

Ru, B., Wong, C.N., Tong, Y., Zhong, J.Y., Zhong, S.S.W., Wu, W.C., Chu, K.C., Wong, C.Y., Lau, C.Y., Chen, I., et al. (2019). Tisidb: an integrated repository portal for tumor-immune system interactions. Bioinformatics *35*, 4200–4202. https://doi.org/10.1093/bioinformatics/btz210.

Ruf, B., Heinrich, B., and Greten, T.F. (2021). Immunobiology and immunotherapy of Hcc: Spotlight on innate and innate-like immune cells. Cell. Mol. Immunol. *18*, 112–127. https://doi.org/10.1038/s41423-020-00572-w.

Stamm, H., Klingler, F., Grossjohann, E.M., Muschhammer, J., Vettorazzi, E., Heuser, M., Mock, U., Thol, F., Vohwinkel, G., Latuske, E., et al. (2018). Immune checkpoints Pvr and Pvrl2 are prognostic markers in Aml and their blockade represents a new therapeutic option. Oncogene *37*, 5269–5280. https://doi.org/10.1038/s41388-018-0288-y.

Tang, Z., Li, C., Kang, B., Gao, G., Li, C., and Zhang, Z. (2017). Gepia: a web server for cancer and normal gene expression profiling and interactive analyses. Nucleic Acids Res. *45*, W98–W102. https://doi.org/10.1093/Nar/Gkx247.

Wang, C., Li, Y., Jia, L., Kim, J.K., Li, J., Deng, P., Zhang, W., Krebsbach, P.H., and Wang, C.Y. (2021). Cd276 expression enables squamous cell carcinoma Stem cells to evade immune Surveillance. Cell Stem Cell *28*, 1597–1613.e7. https://doi.org/10.1016/j.stem.2021.04.011.

Wang, L., Liu, W., Liu, J., Wang, Y., Tai, J., Yin, X., and Tan, J. (2020). Identification of immune-related therapeutically relevant biomarkers in breast cancer and breast cancer stem cells by transcriptome-wide analysis: a clinical prospective study. Front. Oncol. *10*, 554138–554146. https://doi.org/10.3389/fonc.2020.554138.

Wu, Q., Chen, J.X., Chen, Y., Cai, L.L., Wang, X.Z., Guo, W.H., and Zheng, J.F. (2018). The chemokine receptor Ccr10 promotes inflammation-driven hepatocarcinogenesis via Pi3k/Akt pathway activation. Cell Death Dis. *9*, 232. https://doi.org/10.1038/s41419-018-0267-9.

Xia, A., Zhang, Y., Xu, J., Yin, T., and Lu, X.J. (2019). T cell dysfunction in cancer immunity and immunotherapy. Front. Immunol. *10*, 1719–2153. https://doi.org/10.3389/fimmu.2019.01719.

Xu, D., Zhao, E., Zhu, C., Zhao, W., Wang, C., Zhang, Z., and Zhao, G. (2020). Tigit and Pd-1 may serve as potential prognostic biomarkers for gastric cancer. Immunobiology *225*, 151915–152145. https://doi.org/10.1016/j.imbio.2020.151915.

Yu, G.T., Bu, L.L., Zhao, Y.Y., Mao, L., Deng, W.W., Wu, T.F., Zhang, W.F., and Sun, Z.J. (2016). Ctla4 blockade reduces immature myeloid cells in head and neck squamous cell carcinoma. OncoImmunology *5*, 11515944–E1152139. https://doi.org/10.1080/2162402x.2016.1151594.

Zhang, H., Dutta, P., Liu, J., Sabri, N., Song, Y., Li, W.X., and Li, J. (2019). Tumour cell-intrinsic Ctla4 regulates Pd-L1 expression in non-small cell lung cancer. J. Cell Mol. Med. *23*, 535–542. https://doi.org/10.1111/jcmm.13956.

Zhu, H., Wang, G., Zhu, H., and Xu, A. (2021). Mtfr2, A potential biomarker for prognosis and immune infiltrates, promotes progression of gastric cancer based on bioinformatics analysis and experiments. J. Cancer *12*, 3611–3625. https://doi.org/10.7150/jca.58158.

Zhu, M., Xu, W., Wei, C., Huang, J., Xu, J., Zhang, Y., Zhao, Y., Chen, J., Dong, S., Liu, B., and Liang, C. (2019). Ccl14 serves as a novel prognostic factor and tumor suppressor of hcc by modulating cell cycle and promoting apoptosis. Cell Death Dis. *10*, 796. https://doi.org/10.1038/s41419-019-1966-6.

STAR★METHODS

KEY RESOURCES TABLE

REAGENT or RESOURCE	SOURCE	IDENTIFIER
Antibodies		
Mouse monoclonal anti-FAM54A (MTFR2)	Invitrogen	Cat#MA5-27463; RRID: AB_2723165
Rabbit monoclonal anti-PD1	Abcam	Cat#ab137132; RRID:AB_2894867
Rabbit monoclonal anti-PDL1	Abcam	Cat#ab205921; RRID:AB_2687878
Rabbit monoclonal anti-CD8	Abcam	Cat#ab101500; RRID:AB_10710024
Biological samples		
Human HCC and adjacent non-tumor tissues	Xiangya Hospital of Central South University	N/A
Chemicals, peptides, and recombinant proteins		
Trizol	Invitrogen	Cat#10296010
Radioimmunoprecipitation assay buffer	Beyotime	Cat#P0013B
Immobilon Western HRP substrate	Millipore	Cat#WBKLS0500
SYBR Green fluorescent-based assay	TaKaRa Bio Inc.	Cat#638320
Uni All-in-One First-Strand cDNA Synthesis Super-Mix for qPCR	Trans-Script	Cat#AU341-02
Critical commercial assays		
BCA protein assay kit	Beyotime	Cat#P0010
Deposited data		
GEO: GSE212529	NCBI GEO	https://www.ncbi.nlm.nih.gov/geo/query/acc.cgi?acc=GSE212529
Experimental models: Cell lines		
HCC cell lines and human hepatocyte cell line	China Center for Type Culture Collection	N/A
Oligonucleotides		
Primers of MTFR2: Forward:5′-ATTTTGGCGTTCCTGTAGAACA-3′; Reverse: 5′-CAGAGTTCAAGAGCGGGATCA-3′;	This paper	N/A
Primers of GAPDH: Forward:5′-CTGGGCTACACTGAGCACC-3′; Reverse:5′-AAGTGGTCGTTGAGGGCAATG-3′;	This paper	N/A
Software and algorithms		
ImageJ	ImageJ	https://imagej.nih.gov/ij/
GraphPad Prism 7.0	GraphPad	www.graphpad.com
Adobe Illustrator 2020	Adobe	http://aotucad2.xmjfg.com/pg/230.html
Image Lab software	Bio-Rad	www.bio-rad.com
R studio Version 1.2.1335 (R version 3.6.3)	RStudio, Inc.	https://www.rstudio.com/
SPSS 20.0	IBM	https://spss.en.softonic.com/

RESOURCE AVAILABILITY

Lead contact

Further information and requests for resources and reagents should be directed to and will be fulfilled by the lead contact, Hong Shen (hongshen2000@csu.edu.cn).

Materials availability

This study did not generate new unique reagents.

Data and code availability

- The accession number for the RNA-Seq data reported in this paper is in the Gene Expression Omnibus (GEO: GSE212529). The direct link to the data is: https://www.ncbi.nlm.nih.gov/geo/query/acc.cgi?acc=GSE212529.
- This paper does not report original code.
- Any additional information required to reanalyze the data reported in this paper is available from the lead contact upon request.

EXPERIMENTAL MODEL AND SUBJECT DETAILS

Patients, follow-up and Ethics

All patients included were adults over 18 years of age. Tissue samples from 69 patients with hepatocellular carcinoma in Xiangya Hospital of Central South University from September 2014 to February 2019 were collected and fabricated into tissue microarrays. As of Mar 29, 2022, a total of 69 patients were enrolled for a retrospective cohort study. After follow-up, survival analysis, univariate and multivariate cox regression analysis and clinical characteristics analysis were performed. Seven samples from the patients with hepatocellular carcinoma who received anti-PD-1 immunotherapy after the surgery were collected from Xiangya Hospital of Central South University. Clinical data and related pathological features were obtained from the patients' medical records. This study was reviewed and approved by the Medical Ethics Committee of Xiangya Hospital of Central South University.

Cell cultures

Human HCC cell lines Hep3B, HepG2, Huh-7, MHCC97-H, HCCLM3, SMMC-7721, PLC/PRF/5 and normal hepatic cell line L02 were obtained from the Cell Bank of Typical Culture Preservation Committee of Chinese Academy of Science, Shanghai, China. The cells were cultured in high glucose Dulbecco's modified Eagle medium (DMEM) supplemented with 10% fetal bovine serum (FBS) (Gibco, Grand Island, NY), 100 U/mL penicillin sodium and 100 μg/mL streptomycin (Biotechnology, Beijing, China) at 37°C under an atmosphere of 95% air and 5% CO_2.

METHOD DETAILS

Western blot

Total protein was extracted in radioimmunoprecipitation assay buffer (P0013B, Beyotime, Shanghai, China) containing protease inhibitors. The protein concentration was determined using the BCA protein assay kit (Beyotime Biotechnology, Shanghai, China). 20 ug of each protein sample was separated by 10% SDS-PAGE, and then transferred to a 0.2 μm polyvinylidene fluoride (PVDF) membrane (MILLIBOLE, Bedford, MA) under a constant 300 mA. The membrane was sealed in 5% skimmed milk diluted with TBST (Tris-buffered saline with 0.5% Tween) at 37°C for 1 h. Next, the mixture was incubated with the primary antibody (FAM54A(MTFR2): 1:500 dilution; Introvigen, Carlsbad, CA, USA) at 4°C overnight. The mixture was then incubated with HRP-conjugated IgG at 37°C for 1 h and the membrane was washed with TBST. The signal was detected by the enhanced chemiluminescence kit Immobilon Western HRP substrate (WBKLS0500, Millipore), and the ChemiDoc XRS + system (Bio-Rad, Hercules, CA) was used for automatic visualization. Image Lab software (Bio-Rad) was used for the quantitative analysis. The expression of GAPDH protein was used as an internal control. The protein expression levels of MTFR2 in gastric cancer cell lines: GES1, SNU-1, SNU-216, MKN45 and NCI-N87 are used as the positive control (Figure S1A).

Real-time qPCR

Total RNA was extracted using TRIzol reagent (Invitrogen, Carlsbad, CA), and the reverse transcription was performed using uni all-in-One first-strand cDNA synthesis super-Mix for qPCR (Trans-Script, Beijing, China) according to the producer's recommendations. Real-time PCR was performed in triplicate by SYBR Green fluorescent-based assay (638320, TaKaRa Bio Inc.) on a ViiATM7 RT-PCR system (Applied Biosystems, Carlsbad, CA). The primers for real-time PCR were listed as follows: MTFR2: Forward:5′-ATTTTG

GCGTTCCTGTAGAACA-3′; Reverse: 5′-CAGAGTTCAAGAGCGGGATCA-3′; GAPDH: Forward:5′-CTGG GCTACACTGAGCACC-3′; Reverse:5′-AAGTGGTCGTTGAGGGCAATG-3′; Relative mRNA expression levels were calculated by the $2^{-(\Delta\Delta Ct)}$ [Δ Ct = Ct (targeting gene)-Ct (GAPDH)] method and were normalized to the internal control of GAPDH.

Immunohistochemistry (IHC)

HCC tissues were fixed with 10% formalin, dehydrated, paraffin-embedded and prepared into tissue chips to detect MTFR2 protein expression. After dewaxing and hydration, sodium citrate antigen repair solution was used for antigen repair and then endogenous peroxidase was blocked. Normal goat serum was sealed at 37°C for 20 min to reduce non-specific staining. Mouse monoclonal antibody of MTFR2 diluted at 1:150 was then incubated overnight at 4°C. Next biotin-labeled goat anti-mouse IGg was incubated at 37°C for 20 min. DAB and hematoxylin were then used for staining. MTFR2 staining score was defined by both staining intensity score and positive staining percentage score. Dyeing intensity was divided into 4 grades: 0, negative; 1, weakly positive; 2, moderately positive; 3, strongly positive. The percentage of positive staining was divided into 4 groups: 0, negative; 1, positive in 1–25%; 2, positive in 26–50%; 3, positive in 51–75%; 4, positive in 76–100%.

RNA sequencing of immunotherapy cohort

Seven fresh hepatocellular carcinoma samples from the patients who received anti-PD-1 immunotherapy after the surgery were collected from Xiangya Hospital of Central South University and were immediately stored in liquid nitrogen. Total RNA was extracted from the tissues using TRIzol (Invitrogen, Carlsbad, CA, USA) according to the manufacturer's instructions. RNA-sequencing was conducted on the immunotherapy cohort. Raw reads were processed using the Illumina Hiseq. Trimmomatic software was used to perform quality control. The gene expression levels were calculated using reads per kilobase per million reads (RPKM).

Immunotherapy response biomarkers

Neutrophil-to-lymphocyte ratio (NLR) was calculated as absolute neutrophil count/absolute lymphocyte count, derive neutrophil-to-lymphocyte ratio (dNLR) was calculated as absolute neutrophil count/[white blood cell concentration – absolute neutrophil count], lymphocyte to monocyte ratio (LMR) was calculated as absolute lymphocyte count/absolute monocyte count, platelet to lymphocyte ratio (PLR) was calculated as absolute platelet count/absolute lymphocyte count.

Public data source

The Cancer Genome Atlas (TCGA, https://portal.gdc.cancer.gov/): The RNA-Seq data and the clinical information of hepatocellular carcinoma of TCGA were downloaded from the UCSC Xena data portal, the data version is TCGA.LIHC.sampleMap/HiSeqV2 (date: 2017-10-13), Level_3 data. Inclusive criteria: (1). Patients with data of RNA-Seq and contain overall survival time. (2). Patients with more than one tissues will only chose the ID in the survival data to rule out the overlap. (3). The latest version of TCGA follow-up data in UCSC Xena. Exclusive criteria: (1). Patients without survival data. (2). Overlap tissues for same patients.

Processing of RNA-Seq data

All counts, RPKM or fragments per kilobase of transcript per million (FPKM) values were transformed to transcripts per kilobase million (TPM) values under GENCODE annotation (https://www.gencodegenes.org/) version 34 for further analysis. Samples with TPM data were directly used for further analysis.

Evaluation of the immunological characteristics

The data from TIMER, GEPIA and TISIDB (Li et al., 2017; Ru et al., 2019; Tang et al., 2017) were used in the analyses of the correlations between MTFR2 and immune infiltration level/immune regulatory factors. The 19 inhibitory immune checkpoints were obtained from studies by Cai et al., (2022). The immune process steps analyses were conducted by the TIP algorithm.

QUANTIFICATION AND STATISTICAL ANALYSIS

Data processing, analysis, and visualization were performed in R (3.6.3), SPSS 20.0 and GraphPad Prism 7.0. The correlations between variables were explored using Spearman coefficients. Continuous variables fitting a normal distribution between binary groups were compared using a t-test. Otherwise, the Kruskal-Wallis test was applied. ''limma'' package and empirical Bayesian approach were used for performing differential analysis on enrichment results or expression level. Kaplan-Meier curve and log rank test were used to evaluate the prognostic value of MTFR2 for hepatocellular carcinoma. The overall survival (OS) was measured from the date of diagnosis to the date of death or the date of final follow-up, and the final assessment was performed on October 20, 2021. Single factor and multivariate logistic regression analysis were used to determine the influencing factors of MTFR2 expression level (high and low) in HCC. If not specified, a result with a P-value less than 0.05 were considered statistically significant.